HHS Public Access

Author manuscript

Clin Transl Imaging. Author manuscript; available in PMC 2015 August 03.

Published in final edited form as:

Clin Transl Imaging. 2014 August 1; 2(4): 343–358. doi:10.1007/s40336-014-0070-2.

The role of PET quantification in cardiovascular imaging

Piotr Slomka[1,2], **Daniel S. Berman**[1], **Erick Alexanderson**[3,4], and **Guido Germano**[1,2]

[1]Departments of Imaging and Medicine, and Cedars-Sinai Heart Institute, Cedars-Sinai Medical Center, Los Angeles, CA

[2]David Geffen School of Medicine, University of California Los Angeles, Los Angeles, CA

[3]Cardiovascular Imaging & Nuclear Cardiology Department, Instituto Nacional de Cardiología 'Ignacio Chávez', Mexico City, Mexico

[4]Facultad de Medicina, Universidad Nacional Autónoma de México, Mexico City, Mexico

Abstract

Positron Emission Tomography (PET) has several clinical and research applications in cardiovascular imaging. Myocardial perfusion imaging with PET allows accurate global and regional measurements of myocardial perfusion, myocardial blood flow and function at stress and rest in one exam. Simultaneous assessment of function and perfusion by PET with quantitative software is currently the routine practice. Combination of ejection fraction reserve with perfusion information may improve the identification of severe disease. The myocardial viability can be estimated by quantitative comparison of fluorodeoxyglucose (^{18}FDG) and rest perfusion imaging. The myocardial blood flow and coronary flow reserve measurements are becoming routinely included in the clinical assessment due to enhanced dynamic imaging capabilities of the latest PET/CT scanners. Absolute flow measurements allow evaluation of the coronary microvascular dysfunction and provide additional prognostic and diagnostic information for coronary disease. Standard quantitative approaches to compute myocardial blood flow from kinetic PET data in automated and rapid fashion have been developed for ^{13}N-ammonia, ^{15}O-water and ^{82}Rb radiotracers. The agreement between software methods available for such analysis is excellent. Relative quantification of ^{82}Rb PET myocardial perfusion, based on comparisons to normal databases, demonstrates high performance for the detection of obstructive coronary disease. New tracers, such as ^{18}F-flurpiridaz may allow further improvements in the disease detection. Computerized analysis of perfusion at stress and rest reduces the variability of the assessment as compared to visual analysis. PET quantification can be enhanced by precise coregistration with CT angiography. In emerging clinical applications, the potential to identify vulnerable plaques by quantification of atherosclerotic plaque uptake of ^{18}FDG and ^{18}F-sodium fluoride tracers in carotids, aorta and coronary arteries has been demonstrated.

Compliance with Ethics Guidelines: Cedars-Sinai Medical Center receives royalties for the quantitative assessment of function, perfusion, and viability, a portion of which is distributed to some of the authors of this manuscript (DB, GG, PS). The authors declare that they have no conflict of interest. This article does not contain any studies with human or animal subjects performed by any of the authors.

Keywords

cardiac PET; quantification; myocardial perfusion; myocardial perfusion flow; coronary flow reserve; myocardial viability; hybrid PET/CT; cardiac function; vascular imaging; vulnerable plaque

Introduction

Positron emission tomography (PET) allows accurate measurement of relative myocardial hypoperfusion, absolute myocardial blood flow and function at stress and rest, in the same patient study. PET is considered as the gold standard for the myocardial flow reserve measurements. PET is also an important tool in the assessment of the viability of the myocardium. New cardiac PET imaging techniques are being developed to investigate plaque inflammation in the cardiovascular system. The multitude of information, which can be obtained from PET images, necessitates the use of quantitative measurements. Some of the parameters such as absolute blood flow measurements cannot be obtained by visual analysis alone. In addition, quantitative or semi-quantitative analysis of PET data allows reduced observer variability. This review describes PET quantification techniques and summarizes their role as applied to cardiovascular imaging.

Quantification of perfusion and ischemia

PET myocardial perfusion is recommended for diagnosis or risk stratification of patients who have non-diagnostic other imaging tests (1). Cardiac PET/CT provides a highly accurate evaluation for detection of obstructive coronary artery disease (CAD) (2-4) by analysis of perfusion changes between stress and rest (ischemia) and by comparison of perfusion studies to normal limits created from images of subjects with low likelihood of disease and normal scans. The normal limit based quantification technique is widely used in SPECT imaging and has been adapted to PET imaging. Typically an integrated score combining hypoperfusion severity and extent is derived. The quantitative analysis of relative hypoperfusion has been shown to rival the accuracy of the expert readers in diagnosis of coronary artery disease in SPECT in large studies (5). The key advantage of quantitative analysis is the improved reproducibility as compared to even intra-observer variability (6).

In the previous reports of cardiac PET diagnostic performance of perfusion imaging, the average sensitivity for detecting at least one coronary artery with significant stenosis was 89% (range, 83%–100%), whereas the average specificity was 89% (range, 73%–100%) (7) Most of these studies have been obtained with standalone 2D PET scanners rather than with integrated PET/CT systems and utilized visual scoring of perfusion defects in 17-segment model, analogous to SPECT perfusion scoring. Although automated relative quantification was initially developed for SPECT imaging, several recent studies report the use of this method for PET/CT imaging. To date, three studies have reported ^{82}Rb PET/CT diagnostic performance with quantitative analysis method based on the comparison to normal limits (Figure 1) (4, 8, 9). Kaster et al. achieved perfect 100% sensitivity for detection of obstructive CAD when transient ischemic dilation results were also considered in the final result (8). Examples of perfusion images and quantification results both based on normal

limits and on the direct stress-rest comparison for the ^{82}Rb are shown in Figure 2. It should be noted, that due to variable characteristics of normal perfusion distribution for different tracers, for example reduced isotope concentration in the lateral wall for the ^{13}N-ammonia imaging (10), relative analysis of PET perfusion will require isotope-specific normal limits.

Quantification of PET function

The quantitative analysis of myocardial function has been extensively validated for myocardial SPECT (11) but these methods can be also applied to PET. A typical contemporary protocol for PET imaging includes list mode acquisition at stress and rest. This allows the retrospective reformatting and re-binning with cardiac gating and subsequently derivation of functional data. An excellent correlation of MRI and PET ^{18}FDG function analysis for computation of ejection fraction (EF) as well as systolic and diastolic volumes has been reported (12, 13). As compared to SPECT, PET images exhibit higher image resolution and better definition of the mitral valve plane due to accurate attenuation correction (4). This allows implementation of more accurate left ventricular detection of the myocardium and improved tracking of the valve plane. High PET image resolution and ^{18}FDG uptake in the right ventricle may also allow quantification of right ventricular function by PET (14).

PET function analysis can be used in conjunction with perfusion analysis for improved patient risk stratification. In the study including 1441 patients, stress ejection fraction measured from ^{82}Rb PET has provided an independent and incremental prognostic value as compared to perfusion measures (15). The functional measurements from PET may also include phase and dyssynchrony analysis. Although these techniques have not been extensively validated with PET, measurements of histogram bandwidth and phase standard deviation from ^{15}O-water and ^{18}FDG PET scans, were found to be very well correlated with SPECT (16). Recently, in the analysis of 486 patients, left ventricular mechanical dyssynchrony was found to be an independent predictor of all-cause mortality in ischemic cardiomyopathy (17). Furthermore, the analysis of dyssynchrony obtained from the gated ^{18}FDG PET imaging has been shown to identify the responders to cardiac resynchronization therapy (18). Another functional quantitative parameter first described and validated for SPECT, is the transient ischemic dilation of the left ventricle. This measure has been found to improve the identification of patients with severe coronary artery disease in SPECT (19). Rischpler et al. demonstrated the use of the transient ischemic dilation in ^{82}Rb PET imaging as an independent predictor of mortality. (20)

A key advantage of PET perfusion imaging as compared to SPECT is the possibility of immediate imaging during stress. Thus, with PET imaging, it is possible to assess the true peak stress function, unlike in SPECT where scans are performed typically 15-45 minutes after stress. Therefore, PET imaging allows quantifying the EF reserve–defined as the change of the EF between stress and rest. In 510 patients, Dorbala et al. have shown that the EF reserve obtained with ^{82}Rb imaging was the only independent predictor of the left main and 3-vessel disease (21). Very high negative predictive value (97%) for this condition was demonstrated if the EF reserve was higher than 5%. Thus, the ^{82}Rb PET quantification of the left ventricular EF reserve could be used as a tool to exclude the multi-vessel or left main

coronary disease. The same group has further shown that left ventricular EF reserve adds incremental prognostic value as compared to clinical variables and resting EF obtained from ^{82}Rb PET (22). Recently the use of the EF reserve quantification was evaluated for the regadenoson stress agent and ^{82}Rb PET imaging. The mean left ventricular EF reserve was shown to be significantly higher in patients with normal myocardial perfusion imaging results (6.5% ± 5.4%) than in those with mild (4.3% ± 5.1, P = 0.03) and moderate to severe reversible defects (-0.2% ± 8.4%, P = 0.001). Also, the mean left ventricular EF reserve was significantly higher in patients with a low likelihood of CAD (7.2% ± 4.5%, P < 0.0001) (23).

Viability quantification

PET has been considered to be the most sensitive method and the “gold standard” for assessment of myocardial viability (24). The viability of the left ventricle is assessed by PET imaging of glucose metabolism with ^{18}FDG. PET viability imaging is used to identify the patients with significant amount of viable recoverable myocardium. These patients will have a higher likelihood of benefit from revascularization as compared to the patients who do not show such viable tissue. Typically the ^{18}FDG viability imaging is combined with resting PET perfusion scan (using ^{82}Rb or ^{13}N-ammonia tracer) or even resting SPECT scan. Regions which are abnormal at rest scan but are viable (have some glucose uptake) are defined by combined assessment of both scans. If a certain degree of such mismatch between perfusion and viability is detected, it indicates that the patients may benefit from a revascularization procedure. Currently the usual clinical method for detection of such viability patterns is the visual assessment of the mismatch between resting perfusion defect and the ^{18}FDG PET scan. However, visual methods for the identification of mismatch suffer from the usual problems with inter and intra-observer variability. If specific threshold is required for the decision on the intervention-automated quantitative techniques should be considered to ensure objective patient management. To this end, preliminary quantitative techniques which automatically compute the amount of mismatch and scar have been developed (11, 25).

In the first report of the quantitative viability analysis, Beanlands et al. proposed mismatch and scar scores derived from combined perfusion and viability polar maps. These score parameters consider the combination of extent and severity (25). The Cedars-Sinai group has developed an integrated analysis of perfusion and viability in their software. Viability quantification is accomplished as follows: 3D left ventricular contours derived from resting PET or SPECT scans and ^{18}FDG PET images are co-registered in 3D to correct for rotational and positional errors between the two scans, with the methods developed for alignment of stress/rest image pairs (26). Subsequently, the contours derived from the rest perfusion data are applied to the spatially co-registered ^{18}FDG images. Quantification of the viability scores (mismatch and scar regions) is performed after direct image count normalization between the perfusion and viability scans. The method of assigning mismatch and scar scores is based on the approach taken in the PARR-1 study (25), with automatic registration and utilization of normal limits for resting perfusion. The viability analysis is performed in polar coordinates, with computation of scar and mismatch scores for each patient's polar map within the spatial location of the resting perfusion defect, as defined by

Total Perfusion Deficit (TPD) analysis (27). When the normalized perfusion value at a given polar map location is lower than the normalized ^{18}FDG uptake, the mismatch score is calculated from the difference of the two values. The scar score is calculated relative to the normalized ^{18}FDG uptake in each polar map segment. When normalized perfusion exceeds ^{18}FDG uptake, the scar score is assigned a value equal to the normalized perfusion value in that segment. The total scar score in the entire polar map is then computed as the sum of all segmental scar and mismatch scores, and reported as a percentage of the total area of the left myocardium. An example of mismatch and scar quantification is shown in Figure 3.

Quantitative analysis of mismatch and scar has been used in several clinical trials. The original technique developed by Ottawa group has been utilized in PARR-1 and PARR-2 trials (25) (28). The objective of the PARR-1 trial by Beanlands et al.(25) was to determine whether the extent of the viability (mismatch or scar) is related to the amount of recovery of the LV function and to develop a model predicting recovery after revascularization, based on the viability imaging results. They found that the quantitative measure of scar was a significant independent predictor of LV function recovery after revascularization. In a subsequent substudy of PARR-2 trial, the investigators found that in 182 patients with ischemic LV dysfunction, the risk for cardiac death, myocardial infarction or cardiac-related re-hospitalization is reduced when a quantitative mismatch variable is above 7% (28). Quantitative analysis of mismatch and scar was also recently applied by Ubleis et al. (29) in 244 patients to evaluate the prognostic significance of ^{18}FDG PET viability scanning for the prediction of patients with ischemic cardiomyopathy and left ventricular dysfunction. Their analysis has shown that the patients with mismatch greater than 5% (as established by the quantitative software) who did not undergo early revascularization had significantly higher mortality than the group who had similar mismatch (≥ 5%) and did undergo the intervention. This study illustrates the role of quantitative viability imaging in selection of patients for appropriate therapy. It would have been very difficult to derive such definite mismatch thresholds, which can be used to guide therapy, if quantitative analysis was not employed.

Myocardial blood flow and coronary flow reserve quantification

The myocardial blood flow and coronary flow reserve measurements are becoming routinely included in the clinical assessment due to enhanced dynamic imaging capabilities of the latest PET/CT scanners. PET allows noninvasive measurements in units of milliliters of blood per minute, per gram of myocardium. These absolute measurements have been validated against the invasive flow estimates, such as microsphere techniques, in numerous studies. PET is currently the most validated imaging technique for the quantitative evaluation of the myocardial blood flow.

New software tools for are becoming available, which allow quantification of myocardial blood flow at at stress and rest on a more widespread basis. These tools include kinetic models and algorithms to compute myocardial blood flow and coronary flow reserve from kinetic PET data in for ^{13}N ammonia, ^{15}O-water and ^{82}Rb radiotracers. Current tools allow measurements of stress and rest flow in completely automated or in semi-automated fashion. In Figure 4, we show screen-shots of the 3 implementations of software for computation of

myocardial blood flow and coronary flow reserve. The input function is typically obtained from the first-pass blood pool analysis in the left ventricle or left atrium. Segmentation of the left ventricle and determination of the blood pool region can be accomplished automatically. Patient motion correction can be also applied to improve the robustness of the analysis. The computations are rapid, typically accomplished within seconds. Both global and regional or segmental flow and coronary flow reserve measurements are obtained, by kinetic modelling techniques, assuming the appropriate compartmental model, which is specific to a given radiotracer. The inter-scan reproducibility of absolute flow measurement software methods have been reported to be in the order of 15% (30). The quantitative agreement between different software methods available for such analysis is also very good as recently evaluated for ^{82}Rb (31) and ^{13}N-ammonia (32) models (Figure 5). Clinically, ^{82}Rb PET blood flow measurements will have the widest application, since ^{82}Rb does not require a cyclotron on site. Although the ^{82}Rb is not a tracer with ideal imaging properties–for example it has lower extraction fraction than other tracers–the ^{82}Rb flow measurements have been well validated and calibrated to both ^{13}N-ammonia (33) and ^{15}O-water (34) measurements.

Absolute flow measurements and estimation of the myocardial flow reserve allow evaluation of several cardiovascular conditions, which are important clinically. Flow measurements at stress and rest provide the integrated measure of the ischemic burden due to microvascular and macrovascular disease (35). Myocardial flow measurements at stress may allow identification of endothelial dysfunction potentially in early coronary disease (35). In addition, resting myocardial flow heterogeneity and in particular gradient of flow reduction from base to the apex of the left ventricle was demonstrated to be a potential early marker of preclinical coronary artery disease (36). Therefore, these quantitative measurements provide powerful prognostic and diagnostic information, which could be utilized clinically. In Figure 6, we show an example of severely reduced coronary flow reserve in all territories observed in microvascular disease. Relative quantification shows only small abnormality in this case. Patients in which this condition is diagnosed by quantification of myocardial blood flow reserve could benefit from aggressive lipid-lowering therapy (37).

Currently, the diagnosis of the significant, obstructive CAD by PET is typically achieved by visual or quantitative assessment of the relative hypoperfusion at stress and rest rather than by absolute flow quantification. Nevertheless, coronary flow measurements have been shown to be also useful in the diagnosis of CAD, especially in the detection of multivessel CAD. It has been reported that the quantification of ^{82}Rb net retention, to measure the stress-rest blood flow difference in the myocardium, defined a greater extent of disease than the standard quantification based on comparisons of the relative stress and rest perfusion difference (38). Ziadi et al. have studied the incremental value of absolute myocardial flow reserve over standard relative quantification in 120 patients undergoing rest/stress ^{82}Rb imaging. They found that the coronary flow reserve defined by PET is an independent predictor of the 3-vessel CAD and provides added value to the relative quantification by summed stress scoring (39). In a related study by Fietcher et al. (40), absolute measurements of the coronary flow reserve were found to increase the per-patient diagnostic accuracy of ^{13}N-ammonia from 79% to 92% to predict angiographic coronary disease in 73 patients. In Figure 7, we show an example of the ^{82}Rb scan with angiographically confirmed triple-

vessel disease in which only 2 territories are identified as abnormal by relative quantification. These preliminary studies reporting increased diagnostic accuracy for detection of coronary disease with absolute flow measurements when combined with relative quantification will need to be confirmed in larger cohorts, since reduced absolute myocardial flow reserve measurements can be caused by factors other than coronary artery disease, or can be related to non-obstructive disease (35), thus reducing the specificity for the detection of the obstructive disease.

Quantification of coronary flow reserve by PET has been also recently established as an important prognostic tool. Coronary flow reserve measurements have been shown to improve patient risk assessments as compared to relative perfusion measurements (summed stress scoring), and ejection fraction results alone (41). Murthy et al. have shown in a study with a population of 2782 patients, that the incorporation of coronary flow reserve into cardiac death risk assessment resulted in correct reclassification of almost 35% of intermediate-risk patients and significant increase in c-index (from 0.82 to 0.84) In Figure 8 incremental prognostic value of coronary flow reserve as compared to ischemia measures is shown. Based on this evidence, quantitative absolute flow measurements can be used to reclassify risk of the patients as compared to the risk obtained by other PET measures such as relative perfusion abnormality or ejection fraction.

Quantification of new tracers

The practicality of the routine clinical imaging with PET is challenged by the need for the cyclotron on-site for ^{13}N-ammonia and ^{15}O-water imaging, or the need for the generator on-site for ^{82}Rb imaging. In addition, ^{82}Rb imaging tracer does not have optimal imaging characteristics, due to long positron range and low extraction fraction. New imaging tracer Flurpiridaz F 18 has been recently proposed for cardiac PET imaging (42). This tracer exhibits high image contrast in the myocardium, prolonged retention and superior extraction as compared to SPECT tracers (Tc-99m or Tl-201) or ^{82}Rb PET. Cardiac PET imaging with Flurpiridaz F 18 could be performed without cyclotron on site due to relatively long half-life of this tracer. New myocardial blood flow quantification models have been proposed and validated for Flurpiridaz F 18. Sherif et al. have shown that it is possible to estimate absolute flow values by simplified analysis of retention and SUV, due to superior imaging characteristics of this tracer (43). These properties of Flurpiridaz F 18 open new opportunities in the use of absolute quantification since SUV measurements do not require input function. Potentially, this would allow treadmill exercise regimen outside of the scanner. Such simplified techniques may lead to a wider acceptance of the quantitative models. Furthermore, high resolution of F-18 Flurpiridaz images may allow improved quantitative accuracy and may warrant the use of sophisticated techniques eliminating cardiac (44) and patient motion (45) to provide optimal quantitative results. Initial diagnostic validation of Flurpiridaz F 18 diagnostic accuracy was reported to be higher than SPECT with visual scoring in Phase II trial (46). Although not yet reported, it is very likely the quantitative analysis of images obtained with this tracer will provide similarly superior diagnostic results.

PET quantification and hybrid imaging

Virtually all PET scanners delivered today come in hybrid configuration as PET/CT. Many of these systems feature high-end 64-slice CT component, which is capable of state-of-the art CT coronary angiography (CTA). Several groups have investigated the feasibility of improved diagnostic performance, when quantitative PET analysis is augmented with anatomical information from coronary CT angiography. Kajander et al. have studied quantitative combined analysis of ^{15}O-water PET blood flow and coronary CTA (47) They have demonstrated that the combination of quantitative PET and coronary CTA achieves 95% sensitivity and a 100% specificity, allowing higher diagnostic accuracy than either CTA or PET alone. In a similar study, Danad et al., have found that the diagnostic accuracy of quantitative ^{15}O-water PET/CTA is superior to either ^{15}O-water PET or CTA alone for the detection of clinically significant CAD (48).

Combined quantitative analysis of PET and CTA requires perfect alignment of PET and CT scans. This cannot be ensured simply by the patient not moving on the bed, since CT angiography is typically acquired in a different breathing pattern than PET. The alignment can be performed interactively; however, such manual intervention is likely to introduce inter-observer variability to the hybrid imaging results. Nakazato et al. validated a fully automated technique for the alignment of PET and CTA.(49) They found that despite CTA and PET scans being performed without the patient leaving the table, the typical misalignments between PET and CTA were between 14 and 27 mm. The automated software was successful in correction of these misalignments, allowing the combined 3D visualization of coronary vessel anatomy and hypoperfusion. Subsequently, the quantitative results were modified in 11 out of 32 studies based on the co-registration with CT angiography (49). Such 3D fusion of the anatomic and functional scan may allow more precise LV contour and vascular territory adjustment for subsequent quantitative analysis.

Vulnerable plaque quantification

Although not yet clinically applied, PET could also be utilized to characterize atherosclerotic plaque deposits within vessel walls. Elevated macrophage content and associated histological evidence of inflammation are the major hallmarks of ruptured arterial plaques. Among the tracer compounds for imaging of the macrophage accumulation, ^{18}FDG is approved for human scanning and is used extensively for the detection and staging of tumors, and for imaging glucose utilization in viable myocardium (50) (see also previous section). ^{18}FDG is also the most validated PET compound for vulnerable plaque imaging (51). High-end PET/CT with 64-slice CT allows precise anatomical delineation of the plaque and vessels anatomy by CT angiography. PET studies of the plaque inflammation in the carotid vessels (52) and in the aorta (53) have been reported. Due to the high resolution of the new hybrid PET/CT scanners, it is also possible to image coronary arteries. Increased ^{18}FDG signal along the course of coronary arteries in patients with known CAD has been reported, but without direct confirmation that plaques existed at the sites of increased uptake (54). Higher ^{18}FDG signal at culprit plaque sites was shown in patients with acute coronary syndrome (55). Another preliminary study with 64-slice PET/CT also found increased ^{18}FDG uptake at culprit sites of acute myocardial infarction after coronary

stenting (56). The other PET tracer, which can potentially depict coronary plaque biology and is approved for human scanning is ^{18}F-sodium fluoride. Preliminary hybrid PET/CT imaging in coronaries with ^{18}F-sodium fluoride has been demonstrated (57). It has been also shown that the focal arterial inflammation precedes subsequent calcification in the same location: a longitudinal ^{18}FDG-PET/CT study (58).

The quantification of these vascular PET images depicting atherosclerotic plaques presents new challenges. In case of plaque inflammation, small hot spots need to be differentiated from the uptake in other adjacent structures. The level of focal activity may need to be compared in patients with suspected inflammation versus controls, or versus previous studies in monitoring of the disease progression. The analysis techniques are similar to the methods used in oncological imaging for tumor uptake quantification. Typically, standard uptake values (SUV) or target to background ratios are used in the analysis of the vascular plaque uptake (56, 59) (57, 60). The quantification of absolute SUV values may be problematic due to small sizes of plaques and the need for partial volume correction, especially in the coronary vessels. New PET reconstruction techniques, which employ resolution recovery, can aid in the correction of the activity localized in small lesions (61). The regions of interest are most robustly guided by coregistered CT angiography anatomical definition of the plaque boundaries. Although it is possible to judge the tracer uptake in the vasculature by visual grading, the results are highly variable. Quantification of target to background ratios or SUV allows detection of subtle, but significant increases of the tracer concentration in the inflamed plaques. In an example from our study of coronary plaque imaging with PET, we show the quantification of the ^{18}F-FDG plaque uptake in 2 cases with acute coronary syndrome (Figure 9).

Summary

PET cardiovascular imaging is a powerful clinical and research tool. It allows determination of the extent and severity of coronary artery disease, identification of early coronary disease by absolute myocardial flow measurements, detection of viable myocardium, measurement of cardiac function, and potential differentiation of vulnerable plaques from stable plaques. Additional synergistic possibilities exist when coupled with CT angiography. Multitude of clinically relevant cardiovascular imaging parameters can be obtained by PET imaging. Some of these variables are inherently quantitative and it is not possible to use visual analysis for their determination (such as absolute blood flow obtained from dynamic data, phase analysis, or ejection faction and systolic/diastolic volumes obtained from gated data). Other variables such as relative myocardial hypoperfusion, myocardial viability or tracer plaque uptake have been traditionally assessed by visual means, but quantitative methods allow improved reproducibility and potentially also improved accuracy. The quantification of PET scans allows objective determination of the disease likelihood and appropriate risk stratification. Virtually all of the functional and perfusion quantitative parameters can be obtained rapidly (typically in a matter of seconds) from reconstructed tomographic data with minimal interaction. For these reasons, the use of advanced objective quantification methods in cardiovascular PET is becoming an integral part of clinical examinations and represents a primary advantage as compared to other modalities.

References

1. Klocke FJ, Baird MG, Lorell BH, et al. ACC/AHA/ASNC guidelines for the clinical use of cardiac radionuclide imaging--executive summary: a report of the American College of Cardiology/American Heart Association Task Force on Practice Guidelines (ACC/AHA/ASNC Committee to Revise the 1995 Guidelines for the Clinical Use of Cardiac Radionuclide Imaging). Circulation. 2003; 108(11):1404–1418. [PubMed: 12975245]
2. Sampson UK, Dorbala S, Limaye A, Kwong R, Di Carli MF. Diagnostic accuracy of rubidium-82 myocardial perfusion imaging with hybrid positron emission tomography/computed tomography in the detection of coronary artery disease. J Am Coll Cardiol. Mar 13; 2007 49(10):1052–1058. [PubMed: 17349884]
3. Santana CA, Folks RD, Garcia EV, et al. Quantitative (82) Rb PET/CT: development and validation of myocardial perfusion database. J Nucl Med. Jul; 2007 48(7):1122–1128. [PubMed: 17574973]
4. Nakazato R, Berman DS, Dey D, et al. Automated quantitative Rb-82 3D PET/CT myocardial perfusion imaging: normal limits and correlation with invasive coronary angiography. J Nucl Cardiol. Apr; 2012 19(2):265–276. [PubMed: 22203445]
5. Arsanjani R, Xu Y, Hayes SW, et al. Comparison of fully automated computer analysis and visual scoring for detection of coronary artery disease from myocardial perfusion SPECT in a large population. J Nucl Med. Feb; 2013 54(2):221–228. [PubMed: 23315665]
6. Xu Y, Hayes S, Ali I, et al. Automatic and visual reproducibility of perfusion and function measures for myocardial perfusion SPECT. J Nucl Cardiol. Dec; 2010 17(6):1050–1057. [PubMed: 20963537]
7. Beanlands RS, Chow BJ, Dick A, et al. CCS/CAR/CANM/CNCS/CanSCMR joint position statement on advanced noninvasive cardiac imaging using positron emission tomography, magnetic resonance imaging and multidetector computed tomographic angiography in the diagnosis and evaluation of ischemic heart disease--executive summary. Can J Cardiol. Feb; 2007 3(2):107–119. [PubMed: 17311116]
8. Kaster T, Mylonas I, Renaud JM, Wells GA, Beanlands RSB, deKemp RA. Accuracy of low-dose rubidium-82 myocardial perfusion imaging for detection of coronary artery disease using 3D PET and normal database interpretation. J Nucl Cardiol. Dec; 2012 19(6):1135–1145. [PubMed: 22996831]
9. Santana CA, Folks RD, Garcia EV, et al. Quantitative 82Rb PET/CT: Development and Validation of Myocardial Perfusion Database. J Nucl Med. Jun 15.2007 15:15.
10. Klingensmith WC 3rd, Noonan C, Goldberg JH, Buchwald D, Kimball JT, Manson SM. Decreased perfusion in the lateral wall of the left ventricle in PET/CT studies with 13N-ammonia: evaluation in healthy adults. J Nucl Med Technol. Dec; 2009 37(4):215–219. [PubMed: 19914976]
11. Germano G, Kavanagh PB, Slomka PJ, Van Kriekinge SD, Pollard G, Berman DS. Quantitation in gated perfusion SPECT imaging: The Cedars-Sinai approach. J Nucl Cardiol. 2007; 14(4):433–454. [PubMed: 17679052]
12. Schaefer WM, Lipke CS, Nowak B, et al. Validation of an evaluation routine for left ventricular volumes, ejection fraction and wall motion from gated cardiac FDG PET: a comparison with cardiac magnetic resonance imaging. Eur J Nucl Med Mol Imaging. Apr; 2003 30(4):545–553. [PubMed: 12589480]
13. Li Y, Wang L, Zhao SH, et al. Gated F-18 FDG PET for assessment of left ventricular volumes and ejection fraction using QGS and 4D-MSPECT in patients with heart failure: a comparison with cardiac MRI. PLoS ONE. 2014; 9(1):e80227. [PubMed: 24404123]
14. Wang L, Zhang Y, Yan C, et al. Evaluation of right ventricular volume and ejection fraction by gated (18) F-FDG PET in patients with pulmonary hypertension: comparison with cardiac MRI and CT. J Nucl Cardiol. Apr; 2013 20(2):242–252. [PubMed: 23354658]
15. Lertsburapa K, Ahlberg AW, Bateman TM, et al. Independent and incremental prognostic value of left ventricular ejection fraction determined by stress gated rubidium 82 PET imaging in patients with known or suspected coronary artery disease. J Nucl Cardiol. Nov-Dec;2008 15(6):745–753. [PubMed: 18984449]

16. Pazhenkottil AP, Buechel RR, Nkoulou R, et al. Left ventricular dyssynchrony assessment by phase analysis from gated PET-FDG scans. J Nucl Cardiol. Oct; 2011 18(5):920–925. [PubMed: 21671145]
17. AlJaroudi W, Alraies MC, Hachamovitch R, et al. Association of left ventricular mechanical dyssynchrony with survival benefit from revascularization: a study of gated positron emission tomography in patients with ischemic LV dysfunction and narrow QRS. Eur J Nucl Med Mol Imaging. Oct; 2012 39(10):1581–1591. [PubMed: 22699531]
18. Lehner S, Uebleis C, Schussler F, et al. The amount of viable and dyssynchronous myocardium is associated with response to cardiac resynchronization therapy: initial clinical results using multiparametric ECG-gated [18F]FDG PET. Eur J Nucl Med Mol Imaging. Dec; 2013 40(12): 1876–1883. [PubMed: 23903666]
19. Xu Y, Arsanjani R, Clond M, et al. Transient ischemic dilation for coronary artery disease in quantitative analysis of same-day sestamibi myocardial perfusion SPECT. J Nucl Cardiol. Jun; 2012 19(3):465–473. [PubMed: 22399366]
20. Rischpler C, Higuchi T, Fukushima K, et al. Transient ischemic dilation ratio in 82Rb PET myocardial perfusion imaging: normal values and significance as a diagnostic and prognostic marker. J Nucl Med. May; 2012 53(5):723–730. [PubMed: 22492731]
21. Dorbala S, Vangala D, Sampson U, Limaye A, Kwong R, Di Carli MF. Value of vasodilator left ventricular ejection fraction reserve in evaluating the magnitude of myocardium at risk and the extent of angiographic coronary artery disease: a 82Rb PET/CT study. J Nucl Med. Mar; 2007 48(3):349–358. [PubMed: 17332611]
22. Dorbala S, Hachamovitch R, Curillova Z, et al. Incremental prognostic value of gated Rb-82 positron emission tomography myocardial perfusion imaging over clinical variables and rest LVEF. JACC Cardiovasc Imaging. Jul; 2009 2(7):846–854. [PubMed: 19608135]
23. Hsiao E, Ali B, Blankstein R, et al. Detection of obstructive coronary artery disease using regadenoson stress and 82Rb PET/CT myocardial perfusion imaging. J Nucl Med. Oct; 2013 54(10):1748–1754. [PubMed: 23940305]
24. Schinkel AF, Bax JJ, Poldermans D, Elhendy A, Ferrari R, Rahimtoola SH. Hibernating myocardium: diagnosis and patient outcomes. Curr Probl Cardiol. Jul; 2007 32(7):375–410. [PubMed: 17560992]
25. Beanlands RSB, Ruddy TD, deKemp RA, et al. Positron emission tomography and recovery following revascularization (PARR-1): the importance of scar and the development of a prediction rule for the degree of recovery of left ventricular function. J Am Coll Cardiol. 2002 Nov 20; 40(10):1735–1743. 2002. [PubMed: 12446055]
26. Slomka PJ, Nishina H, Berman DS, et al. Automatic quantification of myocardial perfusion stress-rest change: a new measure of ischemia. J Nucl Med. Feb; 2004 45(2):183–191. [PubMed: 14960634]
27. Slomka PJ, Nishina H, Berman DS, et al. Automated quantification of myocardial perfusion SPECT using simplified normal limits. J Nucl Cardiol. Jan-Feb;2005 12(1):66–77. [PubMed: 15682367]
28. D'Egidio G, Nichol G, Williams KA, et al. Increasing benefit from revascularization is associated with increasing amounts of myocardial hibernation: a substudy of the PARR-2 trial. JACC Cardiovasc Imaging. Sep; 2009 2(9):1060–1068. [PubMed: 19761983]
29. Uebleis C, Hellweger S, Laubender RP, et al. The amount of dysfunctional but viable myocardium predicts long-term survival in patients with ischemic cardiomyopathy and left ventricular dysfunction. Int J Cardiovasc Imaging. Oct; 2013 29(7):1645–1653. [PubMed: 23744128]
30. El Fakhri G, Kardan A, Sitek A, et al. Reproducibility and accuracy of quantitative myocardial blood flow assessment with (82) Rb PET: comparison with (13)N-ammonia PET. J Nucl Med. Jul; 2009 50(7):1062–1071. [PubMed: 19525467]
31. Dekemp RA, Declerck J, Klein R, et al. Multisoftware reproducibility study of stress and rest myocardial blood flow assessed with 3D dynamic PET/CT and a 1-tissue-compartment model of 82Rb kinetics. J Nucl Med. Apr; 2013 54(4):571–577. [PubMed: 23447656]

32. Slomka PJ, Alexanderson E, Jacome R, et al. Comparison of clinical tools for measurements of regional stress and rest myocardial blood flow assessed with 13N-ammonia PET/CT. J Nucl Med. Feb; 2012 53(2):171–181. [PubMed: 22228795]
33. Lortie M, B R, Yoshinaga K, Klein R, Dasilva JN, DeKemp RA. Quanitification of myocardial blood flow with 82Rb dynamic PET imaging. Eur J Nucl Med. 2007; 34(11):1765–1774.
34. Prior JO, Allenbach G, Valenta I, et al. Quantification of myocardial blood flow with 82Rb positron emission tomography: clinical validation with 15O-water. Eur J Nucl Med Mol Imaging. Jun; 2012 39(6):1037–1047. [PubMed: 22398957]
35. Schelbert HR. Anatomy and physiology of coronary blood flow. J Nucl Cardiol. Aug; 2010 17(4): 545–554. [PubMed: 20521136]
36. Johnson NP, Gould KL. Clinical evaluation of a new concept: resting myocardial perfusion heterogeneity quantified by markovian analysis of PET identifies coronary microvascular dysfunction and early atherosclerosis in 1,034 subjects. J Nucl Med. Sep; 2005 46(9):1427–1437. [PubMed: 16157524]
37. Baller D, Notohamiprodjo G, Gleichmann U, Holzinger J, Weise R, Lehmann J. Improvement in coronary flow reserve determined by positron emission tomography after 6 months of cholesterol-lowering therapy in patients with early stages of coronary atherosclerosis. Circulation. Jun 8; 1999 99(22):2871–2875. [PubMed: 10359730]
38. Parkash R, deKemp RA, Ruddy TD, et al. Potential utility of rubidium 82 PET quantification in patients with 3-vessel coronary artery disease. J Nucl Cardiol. Jul-Aug;2004 11(4):440–449. [PubMed: 15295413]
39. Ziadi MC, Dekemp RA, Williams K, et al. Does quantification of myocardial flow reserve using rubidium-82 positron emission tomography facilitate detection of multivessel coronary artery disease? J Nucl Cardiol. Aug; 2012 19(4):670–680. [PubMed: 22415819]
40. Fiechter M, Ghadri JR, Gebhard C, et al. Diagnostic value of 13N-ammonia myocardial perfusion PET: added value of myocardial flow reserve. J Nucl Med. Aug; 2012 53(8):1230–1234. [PubMed: 22776752]
41. Murthy VL, Naya M, Foster CR, et al. Improved cardiac risk assessment with noninvasive measures of coronary flow reserve. Circulation. Nov 15; 2011 124(20):2215–2224. [PubMed: 22007073]
42. Maddahi J. Properties of an ideal PET perfusion tracer: new PET tracer cases and data. J Nucl Cardiol. Feb; 2012 19(Suppl 1):S30–37. [PubMed: 22259007]
43. Sherif HM, Nekolla SG, Saraste A, et al. Simplified quantification of myocardial flow reserve with flurpiridaz F 18: validation with microspheres in a pig model. J Nucl Med. Apr; 2011 52(4):617–624. [PubMed: 21441533]
44. Berman DS, Germano G, Slomka PJ. Improvement in PET myocardial perfusion image quality and quantification with flurpiridaz F 18. J Nucl Cardiol. Feb; 2012 19(Suppl 1):S38–45. [PubMed: 22259005]
45. Woo J, Tamarappoo B, Dey D, et al. Automatic 3D registration of dynamic stress and rest (82)Rb and flurpiridaz F 18 myocardial perfusion PET data for patient motion detection and correction. Med Phys. Nov; 2011 38(11):6313–6326. [PubMed: 22047396]
46. Berman DS, Maddahi J, Tamarappoo BK, et al. Phase II safety and clinical comparison with single-photon emission computed tomography myocardial perfusion imaging for detection of coronary artery disease: flurpiridaz F 18 positron emission tomography. J Am Coll Cardiol. Jan 29; 2013 61(4):469–477. [PubMed: 23265345]
47. Kajander SA, Joutsiniemi E, Saraste M, et al. Clinical value of absolute quantification of myocardial perfusion with (15)O-water in coronary artery disease. Circ Cardiovasc Imaging. Nov; 2011 4(6):678–684. [PubMed: 21926262]
48. Danad I, Raijmakers PG, Appelman YE, et al. Hybrid imaging using quantitative H215O PET and CT-based coronary angiography for the detection of coronary artery disease. J Nucl Med. 2013; 54(1):55–63. [PubMed: 23232274]
49. Nakazato R, Dey D, Alexanderson E, et al. Automatic alignment of myocardial perfusion PET and 64-slice coronary CT angiography on hybrid PET/CT. J Nucl Cardiol. Jun; 2012 19(3):482–491. [PubMed: 22419224]

50. Maddahi J, Schelbert H, Brunken R, Di Carli M. Role of thallium-201 and PET imaging in evaluation of myocardial viability and management of patients with coronary artery disease and left ventricular dysfunction. J Nucl Med. Apr; 1994 35(4):707–715. [PubMed: 8151399]
51. Vancraeynest D, Pasquet A, Roelants V, Gerber BL, Vanoverschelde JL. Imaging the vulnerable plaque. J Am Coll Cardiol. May 17; 2011 57(20):1961–1979. [PubMed: 21565634]
52. Rudd JH, Warburton EA, Fryer TD, et al. Imaging atherosclerotic plaque inflammation with [18F]-fluorodeoxyglucose positron emission tomography. Circulation. Jun 11; 2002 105(23):2708–2711. [PubMed: 12057982]
53. Tatsumi M, Cohade C, Nakamoto Y, Wahl RL. Fluorodeoxyglucose uptake in the aortic wall at PET/CT: possible finding for active atherosclerosis. Radiology. Dec; 2003 229(3):831–837. [PubMed: 14593193]
54. Wykrzykowska J, Lehman S, Williams G, et al. Imaging of inflamed and vulnerable plaque in coronary arteries with 18F-FDG PET/CT in patients with suppression of myocardial uptake using a low-carbohydrate, high-fat preparation. J Nucl Med. Apr; 2009 50(4):563–568. [PubMed: 19289431]
55. Rogers IS, Nasir K, Figueroa AL, et al. Feasibility of FDG imaging of the coronary arteries: comparison between acute coronary syndrome and stable angina. JACC Cardiovasc Imaging. Apr; 2010 3(4):388–397. [PubMed: 20394901]
56. Cheng VY, Slomka PJ, Le Meunier L, et al. Coronary arterial 18F-FDG uptake by fusion of PET and coronary CT angiography at sites of percutaneous stenting for acute myocardial infarction and stable coronary artery disease. J Nucl Med. Apr; 2012 53(4):575–583. [PubMed: 22419753]
57. Dweck MR, Chow MW, Joshi NV, et al. Coronary arterial 18F-sodium fluoride uptake: a novel marker of plaque biology. J Am Coll Cardiol. 2012; 59(17):1539–1548. [PubMed: 22516444]
58. Abdelbaky A, Corsini E, Figueroa AL, et al. Focal arterial inflammation precedes subsequent calcification in the same location: a longitudinal FDG-PET/CT study. Circ Cardiovasc Imaging. Sep; 2013 6(5):747–754. [PubMed: 23833282]
59. Rogers IS, Tawakol A. Imaging of coronary inflammation with FDG-PET: feasibility and clinical hurdles. Curr Cardiol Rep. Apr; 2011 13(2):138–144. [PubMed: 21274660]
60. Joshi NV, Vesey AT, Williams MC, et al. F-fluoride positron emission tomography for identification of ruptured and high-risk coronary atherosclerotic plaques: a prospective clinical trial. Lancet. Nov 8.2013
61. Panin VY, Kehren F, Michel C, Casey M. Fully 3-D PET reconstruction with system matrix derived from point source measurements. IEEE Trans Med Imaging. Jul; 2006 25(7):907–921. [PubMed: 16827491]

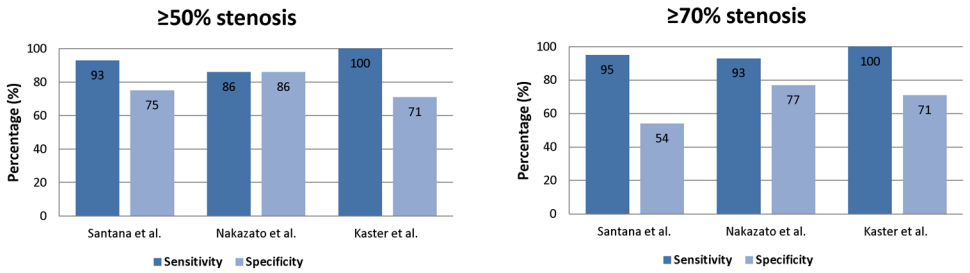

Fig. 1.

Relative quantification accuracy. Results from three recent manuscripts by Santana et al. (3) (n=76), Nakazato et al. (4) (n=167), and Kaster et al.(8) (n=110), validating the use of relative quantification with normal limits for myocardial perfusion PET for detection of coronary artery disease by three separate software tools.

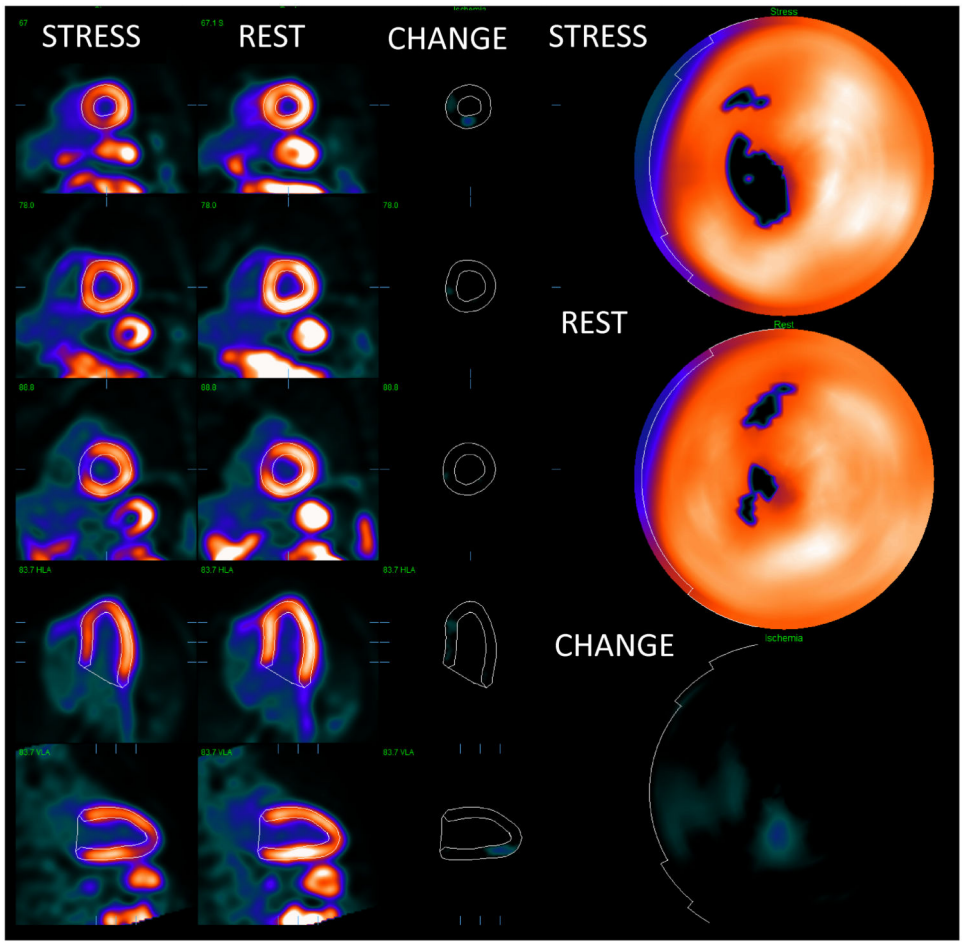

Fig. 2.

An example of relative quantification for myocardial perfusion PET. Co-registered stress and rest images with contours are shown on the left. The change images (CHANGE) in the middle show the ischemic region in the septal wall. Polar maps (right) shows corresponding significant defect on stress. The quantification results were stress TPD=10%, rest TPD=4%, ischemia by change analysis 5%. Ejection fraction was normal. This patient had significant > 70% lesion in the proximal LAD territory as confirmed by angiographic examination.

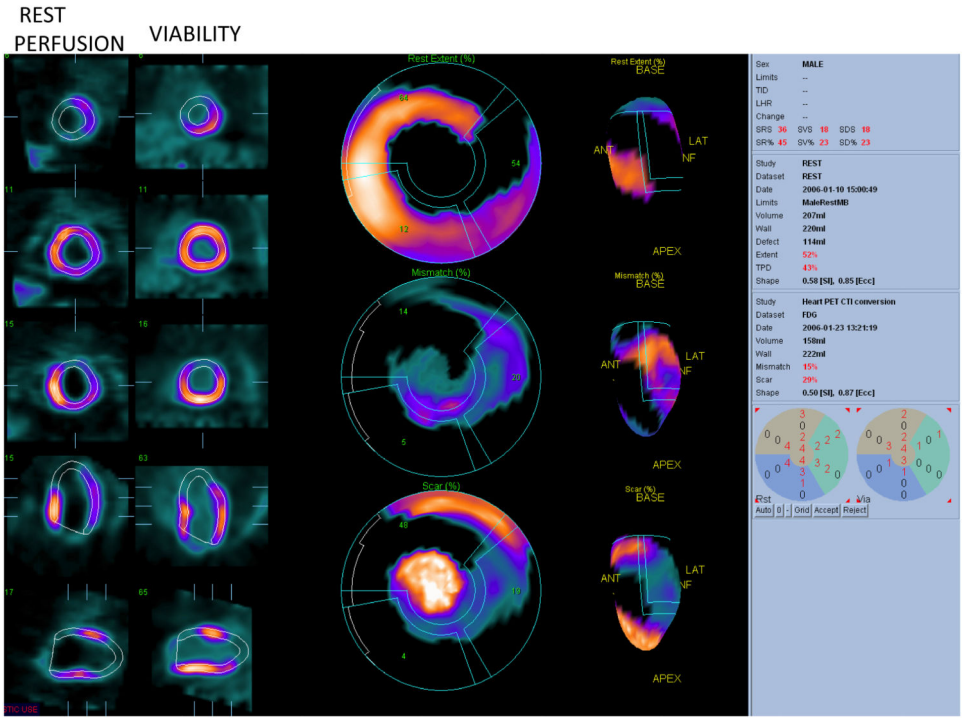

Fig. 3.

Viability quantification. Rest perfusion images and viability images are shown (2 right columns). Polar map quantification (middle column and 3D representation right column) shows resting perfusion defect with Total Perfusion deficit of 43% (top polar map) Mismatch of 15% (middle polar map) and scar of 29% (bottom polar map). Data courtesy Dr. Die Bondt.

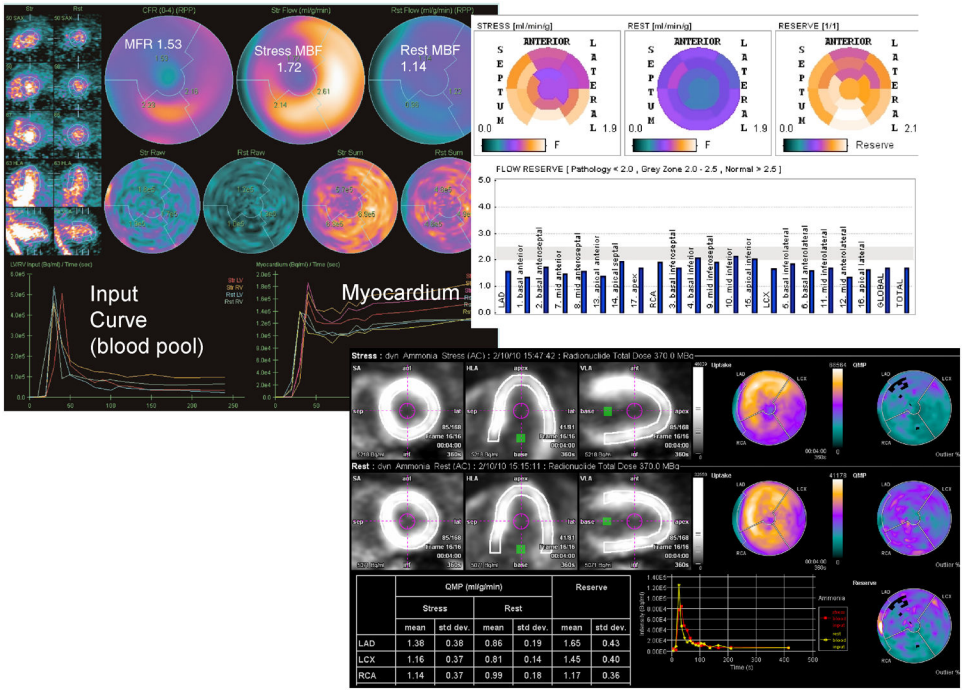

	QMP (ml/g/min)				Reserve	
	Stress		Rest			
	mean	std dev.	mean	std dev.	mean	std dev.
LAD	1.38	0.38	0.86	0.19	1.65	0.43
LCX	1.16	0.37	0.81	0.14	1.45	0.40
RCA	1.14	0.37	0.99	0.18	1.17	0.36

Fig. 4.

Results from different implementations of the absolute flow quantification methods demonstrating regional and segmental quantification of rest and stress myocardial blood flow and coronary flow reserve (CFR). Cedars Sinai QPET (top left) PMOD software (top right) and Siemens syngoMBF flow analysis (bottom) are shown.

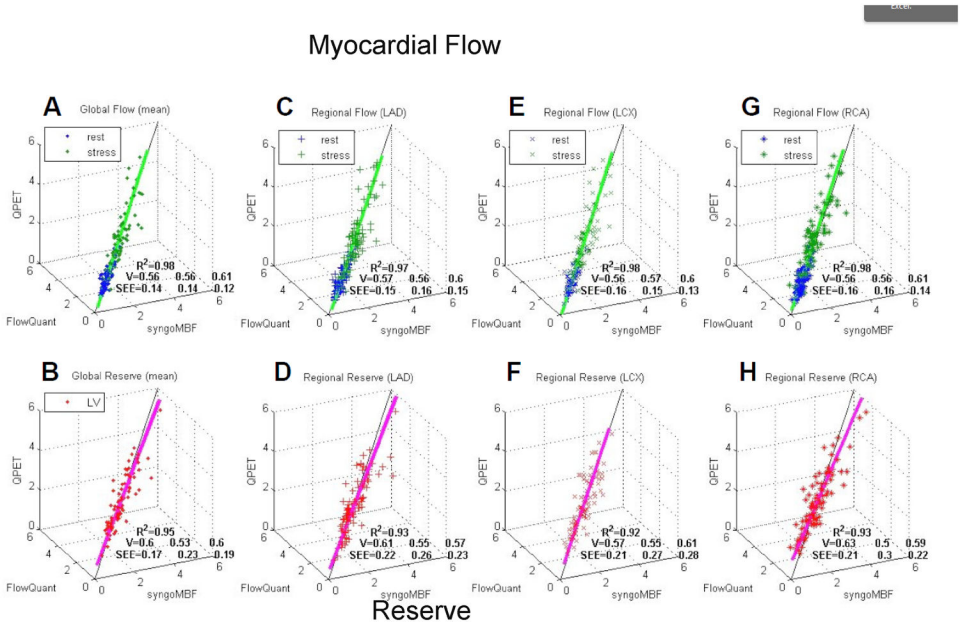

Fig. 5.

Agreement for the software packages on measurements of myocardial blood flow and coronary flow reserve (CFR). 3D scatterplots of syngoMBF vs. FlowQuant vs. QPET values of rest and stress myocardial blood flow and CFR (reserve) for global left ventricle (A and B) and regional vascular territories (C–H). R^2 is total variance described by 3D unit basis vector (V) line of best fit. SEE is standard deviation of residual errors from regression line of best fit for each of the 3 programs. Reproduced with permission from De Kemp et al. (31).

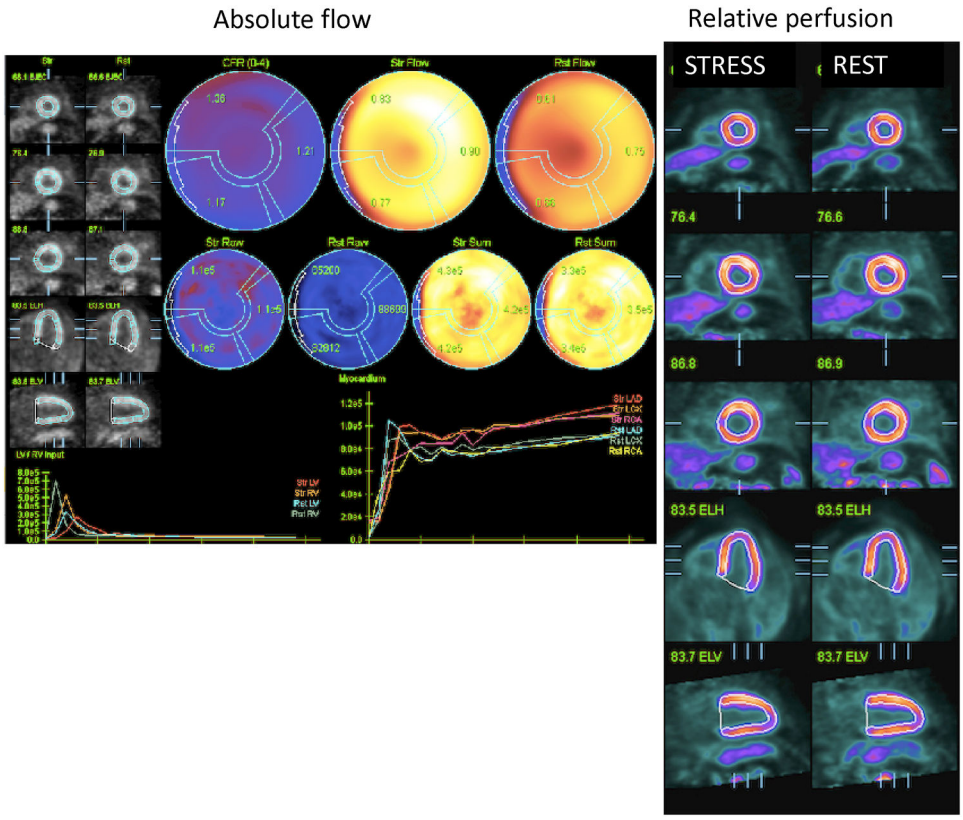

Fig. 6.

Example of severely reduced coronary flow reserve (CFR) (1.17-1.37) and reduced stress flow (0.83-0.77 ml/g/min) in all vascular territories in a patient with syndrome × (left). This patient had borderline abnormal relative perfusion scan with mildly decreased uptake at stress in the part of the inferior wall (right).

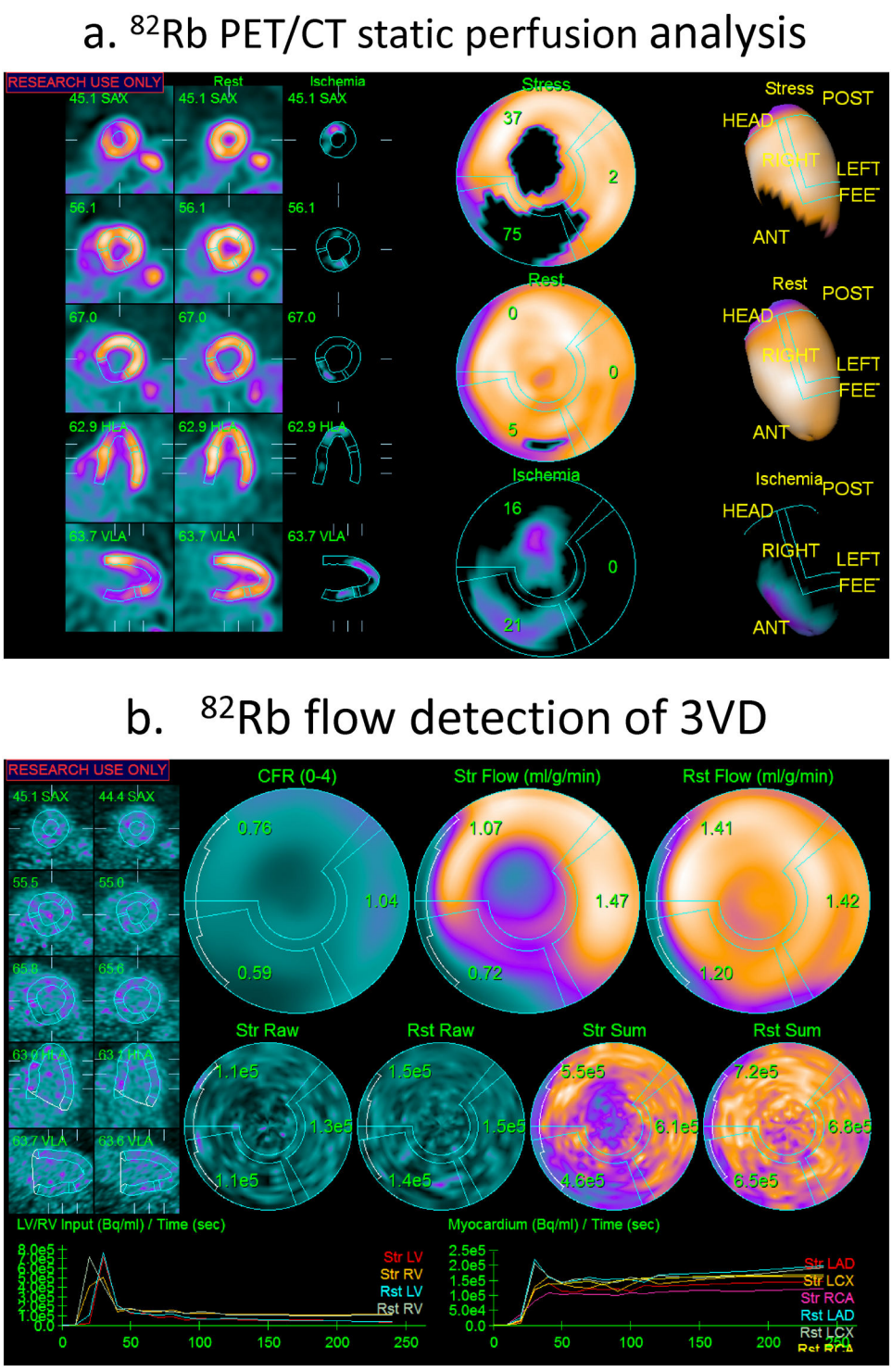

Fig. 7.

Example of added value of myocardial flow reserve over ischemia quantification for diagnosis from ^{82}Rb PET. Relative quantification of total perfusion deficit at stress and rest shows stress and ischemic abnormalities in left anterior descending (LAD) and left circumflex (LCX) territories but normal right coronary artery (RCA) territory (a), while

myocardial flow reserve is definitely abnormal in all vascular territories (0.76-1.04), with no flow reserve (CFR=1.04) in the RCA region (b). This case was angiographically confirmed as triple vessel disease.

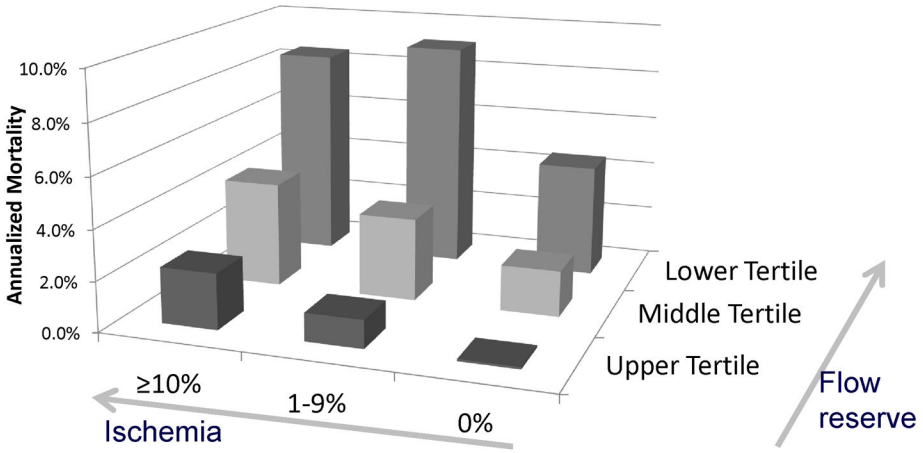

	≥10%	1-9%	0%
Upper Tertile	2.2%	1.1%	0.1%
Middle Tertile	4.2%	3.3%	1.8%
Lower Tertile	8.5%	9.1%	4.5%

Fig. 8.

Incremental prognostic value of coronary flow reserve (CFR) as compared to ischemia measures. Unadjusted annualized cardiac mortality by tertiles of CFR and by categories of myocardial ischemia. The annual rate of cardiac death increased with increasing summed stress score and decreasing CFR. Importantly, lower CFR consistently identified higher-risk patients at every level of myocardial scar/ischemia including among those with visually normal positron emission tomography scans and normal LV function. Reproduced with permission from Murthy et al. (41).

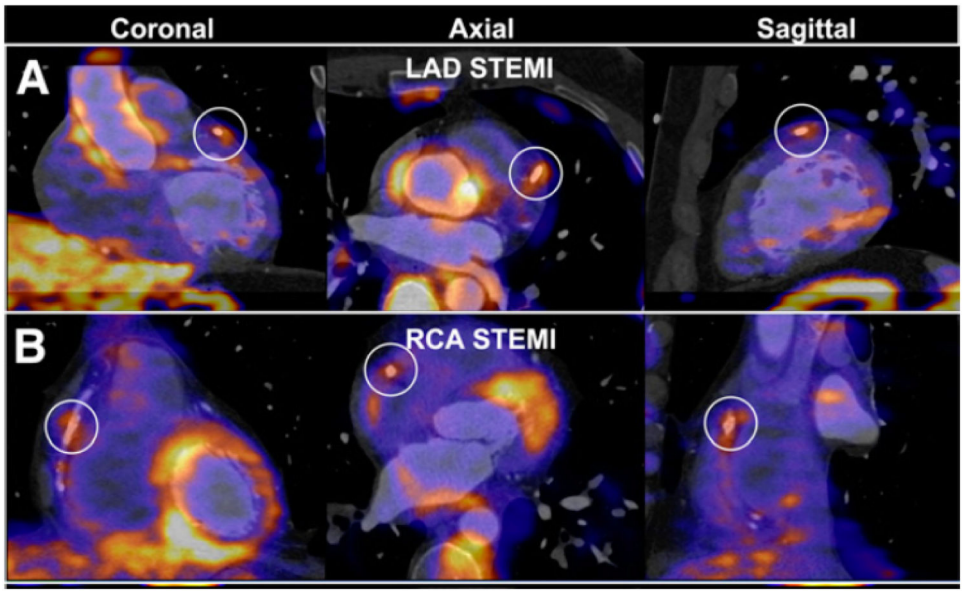

Fig. 9.

PET ^{18}FDG coronary uptake quantification. Examples of increased ^{18}FDG uptake at stent site in patients with acute ST elevation myocardial infarction (STEMI). (A) A 54-y-old man imaged after percutaneous coronary stenting of proximal left anterior descending artery (LAD) for STEMI. Quantification of maximum target-to background ratio (maxTBR) at stent site was 2.1 (white circles). (B) A 49-y-old man imaged after stenting of proximal RCA for STEMI. maxTBR at stent site was 2.1. Reproduced with permission from Cheng et al. (56).